Title

A Kinetic Model of GPCRs: Analysis of G protein Activity, Occupancy, Coupling and Receptor-State Affinity Constants

Journal

The FASEB Journal, 29(S1)

ISSN

0892-6638

Authors

Stein, Richard
Ehlert, Frederick

Publication Date

2015-04-01

DOI

10.1096/fasebj.29.1_supplement.935.1

Peer reviewed

A Kinetic Model of GPCRs: Analysis of G protein Activity, Occupancy, Coupling and Receptor-State Affinity Constants

Journal:	*Journal of Receptors and Signal Transduction*
Manuscript ID:	LRST-2014-0092
Manuscript Type:	Original Paper
Date Submitted by the Author:	22-Jul-2014
Complete List of Authors:	Stein, Richard; University of California, Irvine, Department of Pharmacology Ehlert, Frederick; University of California, Irvine, Pharmacology
Keywords:	active state affinity constant, constitutive activity, GTPase activity, guanine nucleotide, inverse agonism, quaternary complex

A Kinetic Model of GPCRs: Analysis of G protein Activity, Occupancy, Coupling and Receptor-State Affinity Constants

Richard S.L. Stein and Frederick J. Ehlert

Department of Pharmacology, School of Medicine

University of California

Irvine, CA 92697-4625

Corresponding author: Frederick J. Ehlert

Department of Pharmacology

School of Medicine

University of California, Irvine

Irvine, CA 92697-4624

Tel: 949-824-6208

FAX: 949-824-4855

fjehlert@uci.edu

Keywords: Active state affinity constant, constitutive activity, GTPase activity, guanine nucleotide, inverse agonism, quaternary complex

ABSTRACT

Context: G protein-coupled receptors are vital macromolecules for a wide variety of physiological processes. Upon agonist binding these receptors accelerate the exchange of GDP for GTP in G proteins coupled to them. The activated G protein interacts with effector proteins to implement downstream biological functions.

Objective: We present a kinetic, quaternary complex model, based on a system of coupled linear first-order differential equations, that accounts for the binding attributes of the ligand, receptor, G protein and two types of guanine nucleotide (GDP and GTP) as well as for GTPase activity.

Methods: We solved the model numerically to predict the extents of G protein activation, receptor occupancy by ligand, and receptor coupling that result from varying the ligand concentration, presence of GDP and/or GTP, the ratio of G protein to receptor, and the equilibrium constants governing receptor pre-coupling and constitutive activity. We also simulated responses downstream from G protein activation using a transducer function.

Results: Our model provides an explanation for agonist-induced increases or decreases in receptor-G protein coupling coincident with G protein activation. In addition, we demonstrate that affinity constants of the ligand for both the active and inactive states of the receptor can be derived to a close approximation from analysis of simulated responses downstream from receptor activation.

Discussion and conclusion: The latter result validates our prior methods for estimating the active state affinity constants of ligands and our results on receptor coupling have relevance to studies investigating receptor-G protein interactions using fluorescence techniques.

INTRODUCTION

G protein-coupled receptors (GPCRs) participate in nearly all physiological processes and are central to the pathogenesis and treatment of many conditions. These receptors mediate their effects through two classes of proteins, arrestins and G proteins (1, 2). A better understanding of how these pathways are activated and of how agonists bias signaling through one pathway relative to the other would greatly facilitate the identification more selective drugs in pharmacological screening assays.

A number of equilibrium models for receptor-G protein interactions have been described (3) that address single (4) and multiple (5) active and inactive receptor states as well as those of the G protein and an allosteric receptor site (6). These schemes have been useful in explaining the observed affinity and efficacy of agonists and in validating methods for estimating the receptor state affinity constants of agonists, inverse agonists and allosteric ligands (6). It might seem inappropriate to use an equilibrium approach for this purpose because agonist-receptor binding induces GTPase activity that continuously drives a G protein cycle involving the hydrolysis of GTP to GDP followed by the exchange of GTP for GDP. G protein cycling is not expected to alter ligand binding to the receptor, however, because both GTP and GDP have nearly the same effects on agonist binding (7-9). Thus, these models have been useful in the analysis of ligand-receptor interactions despite their lack of coverage of the G protein cycle.

Several investigators have described kinetic models of receptor-G protein interactions that address GTPase activity (10) and states of the receptor (11). The predictions derived from these models regarding the concentration-response curves of agonists for activating G proteins are generally consistent with equilibrium models. Models that describe arrestin recruitment and their output pathways have also been useful in assessing agonist bias (12, 13).

Receptor-G protein interactions have been studied in living cells using fluorescence resonance energy transfer (FRET). In experiments by Hein and coworkers (14, 15) fluorescent molecules were placed in both the receptor and G protein. In this paradigm, excitation of the

donor fluorophore in the G protein causes a FRET signal whenever the acceptor fluorophore on the C-terminus of the receptor is in close proximity. In a related technique known as bioluminescence resonance energy transfer (BRET), the donor fluorophore is replaced with a light emitting luciferase (16, 17). Agonist-induced increases in resonance energy transfer have been interpreted as evidence of an increase in receptor-G protein coupling (14, 15). In some instances, expression of the tagged receptors and G proteins leads to a constitutive BRET signal, suggesting pre-coupling of receptors and G proteins (16, 17). Agonists of the α_{2A} receptor have been observed to increase or decrease the constitutive BRET signal, depending on the location of the luciferase in $G\alpha_i$. Audet and coworkers (17) have suggested that the agonist-induced decrease in BRET can been explained by conformational changes in the interacting proteins that distance the luminescent and fluorescent probes without reducing the amount of preformed receptor-G protein complex.

In this report, we describe and evaluate a complete model for receptor-G protein interactions that includes GTPase activity, active and inactive states of the receptor, and three conformations of the G protein – an inactive state, an exchange state and a dissociated active state. Our model provides an explanation for agonist-induced increases or decreases in receptor-G protein coupling coincident with G protein activation. We have also used the model to validate our prior methods for analyzing functional responses to yield receptor state affinity constants of agonists and inverse agonists.

METHODS

Kinetic Model

The kinetic model was created by stipulating interactions among the following molecules: (a) receptor, which could be in either an active (R*) or inactive (R) state, (b) G protein, which could be in an inactive (G), exchange (G*) or active (G**) state, (c) agonist, (d) GDP, and (e) GTP. The possible complexes presumed to be able to form are agonist with receptor, receptor with G protein, and G protein with GDP or GTP. Population movement between different states of complexation was governed by a system of 173 coupled first-order linear differential equations, stipulating the rates of association and dissociation of the various molecules in the model (Fig. 1, Tables 3–7). Each possible movement between states was assumed to be reversible except for the conversion of GTP bound to the active state of the G protein into GDP (GTPase activity) and the reassembly of the split, inactive Gα and Gβγ subunits back into the holoprotein. At the initial state, all of the receptors are assumed to be unoccupied and uncomplexed with G protein, and all G protein to be bound with GDP (except for conditions where GDP is absent, in which case no G protein was bound with guanine nucleotide). The integration of the differential equations was implemented by the forward Euler method, with a time step of 125 ns, except in the cases where GTP was in the system without GDP, when the Runge-Kutta method was used with a time step of 25 μs. Because of the fast processes involving GDP when it was present in the system, stability issues nullified the advantage of the Runge-Kutta method, making it impractical to implement in those cases.

For all simulations involving receptor activity, the model contained 10^4 receptors and either an equivalent number of G proteins (equal ratio) or approximately 5.6-fold greater (high ratio, i.e., 56,234 G protein molecules). Whenever present the concentrations of GTP and GDP were 4.5×10^{-4} M and 1.5×10^{-4} M, respectively. These values are similar to average estimates measured in a variety of cells (18).

To simulate the resting state, the model was first run in the absence of agonist to allow the system to reach a steady state. To confirm the robustness of the model, we verified for one set of conditions that the system eventually reaches the same steady state when all G protein is initially complexed with GTP (see Fig. 2). For all sets of conditions, this initial resting steady state was then used as the starting point for runs featuring agonist present in a variety of concentrations, typically ranging from 10^{-8} up to 10^{-2} M. The condition of reaching steady state or equilibrium was defined by the population of no state varying by more than 0.001 molecule in 1 sec of simulated time.

For simulations involving significant constitutive receptor activity, the resting state was determined as described above. In addition, the steady state for the case of a lack of receptors was also determined (basal G protein activation). The difference between the estimates of G protein activation for the resting state and basal G protein activation is defined as constitutive activity.

The mechanics of the model can be defined by a set of equilibrium constants: K_a, K_b, K_i, K_j, K_k, K_q, K_p, K_v, K_x, K_y, and K_{act} (see Table I) and associated forward and reverse rate constants. The reverse rate constants for all processes were calculated from the equilibrium and forward rate constants. For example, values of k_{-a} were calculated from K_a and k_a ($k_{-a} = k_a/K_a$). The hydrolysis of GTP to GDP on the active G protein was governed by the single rate constant k_{GTP}. The constants K_q and K_p correspond to the isomerization of the completely free receptor and G protein respectively. Microscopic reversibility was maintained as described in Appendix.

The model was simulated for a variety of conditions. In the "standard system", the conditions for "high-pre-coupling" and "low constitutive activity" as described in Table I were used, the ratio of G protein to receptor was 1:1 (10^4 molecules each), and the rate of GTPase activity k_{GTP} was 0.25/s. Tables I and II contain the parameters K_b and K_a for agonist binding. Table II shows the system variations that were simulated, and the differences from the standard system in each case. For any system with no GDP, any GTP present was non-hydrolyzable, so that k_{GTP} was zero.

The complete set of rate constants for the kinetic model is given in Tables 3–7 of the Appendix (standard system conditions). When possible, rate constants were taken from the system described in ref. (11). Whenever an equilibrium constant was adjusted, the forward rate constant was conserved, so that only the reverse rate constant was changed to reflect the new equilibrium condition.

For all of the simulated systems, the populations of all species at steady state were obtained. These populations were used to calculate the G protein activation, receptor occupancy, and GPCR coupling as functions of agonist concentration. The G protein activation was defined as the fraction of G protein active and bound by GTP, i.e. in the form of the species G**α_{GTP}.

Analysis of simulated ligand concentration-response data

We simulated downstream functional responses to orthosteric ligands by substituting the estimates of G protein activation for the stimulus variable (S) in the transducer function of the operational model (19):

$$Y = \frac{M_{sys}}{1 + \left(\frac{K_E}{S}\right)^m} \qquad 1$$

In this equation, M_{sys} denotes the maximum response of the signaling pathway, K_E, the sensitivity constant, and m, the transducer slope factor. To assess the feasibility of determining relative and absolute estimates of the affinity constants of orthosteric ligands for the active state of the receptor, we analyzed the simulated concentration response curves by nonlinear regression analysis using the equations described below as described previously (5, 20, 21).

For the case of no measureable constitutive activity, the following equation was fitted to the simulated concentration-response curve of the most efficacious orthosteric ligand (standard agonist):

$$Y = \frac{M_{sys}}{1 + \left(\frac{1 + DK_{obs}'}{D * R}\right)^m} \qquad 2$$

In this equation, Y represents the simulated response, D, the concentration of standard agonist, K', its observed affinity constant (units of M^{-1}), and R, the product of K' and τ'. Apostrophes are used to denote the parameters of the standard agonist. The parameter τ is proportional to the efficacy of the ligand (ε) (i.e., $\tau = \varepsilon R_T/K_E$, in which R_T denotes the total receptor concentration). The simulated concentration-response data of the less efficacious ligands (test ligands) were analyzed using the following equation:

$$Y = \frac{M_{sys}}{1+\left(\frac{1+DK_{obs}}{D*R*RA_i}\right)^m} \qquad 3$$

In this equation, RA_i (intrinsic relative activity) denotes the product τK_{obs} for the test ligand divided by that of the standard agonist ($\tau' K_{obs}'$). RA_i is also equivalent to the corresponding ratio of active state affinity constants (K_b/K_b'). Global nonlinear regression analysis was done fitting equations 2 and 3 to the simulated data for the standard and test agonists, respectively. The estimates of M_{sys}, m and R were shared among the ligands and individual estimates of K_{obs} and RA_i were obtained for each test agonist.

For the case of constitutive activity, the following equation was fitted to the simulated concentration-response curves:

$$Y = \frac{M_{sys}}{1+\left(\frac{1+DK_{obs}}{\tau_{sys}\left(1+DK_b\right)}\right)^m} \qquad 4$$

In this equation, τ_{sys} represents a parameter proportional to the constitutive activity of the receptor. Global nonlinear regression analysis was done sharing the estimates of M_{sys}, m and τ_{sys} among the data and obtaining individual estimates of K_{obs} and K_b for each ligand.

RESULTS

Simulation of Receptor-G Protein Interactions

Standard system: The simulated data for the standard system at various values of k_{GTP} (GTPase activity) are shown in Fig. 3. As expected, the activity level, expressed as molecules of free $G\alpha^{**}_{GTP}$ increases with agonist concentration, as well as with decreasing k_{GTP} (Fig. 3*a*). This inverse dependence on k_{GTP} is explained by a higher rate of GTPase activity, which converts active G protein back into G_{GDP}. Receptor occupancy (summation of the various states of the DR, DRG, DRG_{GTP} and DRG_{GDP} complexes) by agonist shows virtually no dependence on the value of k_{GTP} (Fig. 3*b*). Lower values of k_{GTP} lead to lower receptor-G protein coupling (summation of the various states of the RG, RG_{GDP}, DRG and DRG_{GTP} and DRG_{GDP} complexes) in the presence of agonist, particularly in the case where GTPase activity is turned completely off (Fig. 3*c*). The removal of GTPase activity causes a considerable rise in G protein activation (Fig. 3*a*), and hence, a corresponding reduction in the form of the G protein (G_{GDP}) that readily couples to the GPCR.

To obtain activity levels reflecting downstream responses corresponding to specified amounts of G protein activation, the agonist-induced activities illustrated in Figure 3*a* were substituted into the transducer function of the operational model (equation 1, with K_E = 50 molecules and m = 1) to yield the concentration-response curves illustrated in Fig. 3*d*. Further analysis of these concentration-response curves is described below.

Fig. 4 shows the effects of removing one or both of GTP and GDP from the standard system for the condition of no GTPase activity. When both GTP and GDP are present (but GTP is non-hydrolyzable), the activity ranges from 1.44% for [D] = 10^{-8} M to nearly 46% for [D] = 10^{-2} M. In the absence of GDP, the basal activity leaps to 80.95% and drops very slightly to 80.45% at high agonist concentration (Fig. 4*a*). The high activity in the latter case is expected, as GDP serves as a barrier to G protein activity, which is free to surge when GDP is removed from the system.

All conditions with at least one of GDP or GTP exhibit roughly the same agonist binding (Fig. 4*b*), while the absence of all guanine nucleotide considerably increases binding, shifting the occupancy curve leftwards by 1.6 log at half-maximal occupancy. Furthermore, the Hill slope of the resulting occupancy curve is only 0.756, while those for the various guanine nucleotide conditions exhibit values between 0.99 and 1. These results reflect the negative cooperativity between the binding of agonist and guanine nucleotide to the receptor-G protein complex. In the absence of guanine nucleotides, the interaction is determined by the positive cooperativity between the binding of agonist and free G protein. This positive allosteric effect is reduced at moderate to high levels of agonist receptor occupancy (low Hill slope) because the G protein is limiting (R/G = 1.0) in this case (Fig. 4*b*).

When both GDP and GTP are present GPCR coupling falls from 22.8% to 8.0% with increasing agonist concentration (Fig. 4*c*); the coupling rises from 23.4% to 28.6% with GDP only, and from 1.2% to 1.8% with GTP only. In the absence of all guanine nucleotide the coupling increases greatly, from 25.6% for [D] = 10^{-9} M to 91.1% for [D] = 10^{-3} M. We have quantitatively replicated the GPCR coupling for the GDP-only system with an equilibrium model (6).

Excess G protein: The effect of introducing excess G protein into the system, by a ratio of 5.6 molecules for each GPCR, is shown in Fig. 5. There is a large increase in G protein activation in the presence of GTPase activity (Fig. 5*a*), with 1060 G protein molecules activated at high agonist concentration due to receptor influence compared to only 394 when the GPCR ratio is 1:1. The G protein activation without GTPase activity also increases to 6843 molecules compared to 4594 when the GPCR ratio is 1:1. In the absence of GDP, the G protein activity can be seen to decrease noticeably, from 7274 molecules for [D] = 10^{-8} M to 6841 for [D] = 10^{-2} M. A possible explanation for this unexpected phenomenon is that agonist binding causes an increase in GPCR coupling, which would subtract from the G protein activation rate in the GTP-only system.

The occupancy profiles for the various combinations of guanine nucleotide are similar, except in the case of a lack of both GDP and GTP (Fig. 5*b*), when the GPCRs become more sensitive by 2.1 logs to agonist binding. The abundance of G proteins leads to a far higher basal coupling level (78%, versus 23% for the 1:1 GPCR ratio). The GPCR coupling is seen to decrease in the GTPase system from 78.8% for [D] = 10^{-8} M to 68.9% for [D] = 10^{-2} M (Fig. 5*c*). As this is not observed for the 1:1 GPCR ratio, we postulate that the greater activity allowed by the excess of G protein leads to the observed decrease in coupling. With no GTPase activity, the drop in coupling is dramatic (77.3% for [D] = 10^{-8} M to 14.1% for [D] = 10^{-2} M), corresponding with the increase in G protein activation. With only GDP present the coupling increases with agonist addition from 79.1% to 84.0% (11.2% to 16.4% for GTP only, and 81.3% to 99.9% for neither guanine nucleotide).

Low pre-coupling system: Fig. 6 shows the activity, occupancy and coupling data for the above system but with the "low-pre-coupling" condition imposed. Maximum agonist-induced activity for the GTPase system decreases slightly, from 1060 molecules to 796, and in the absence of GTPase activity, from 6843 to 6627 molecules (Fig. 6*a*). Without GDP the activations run greater than for the high-pre-coupling system, from 8190 molecules without ligand to 7411 at high agonist concentration, most likely due to additional G proteins available for activation because of reduced pre-coupling.

Unlike the high-pre-coupling systems, there are small variations in the occupancy profiles of the systems with at least one guanine nucleotide, with an EC_{50} range width of about 0.45 log, and the GDP-only system showing the most binding while the high-activity systems (GTP-only and $k_{GTP} = 0$) exhibit the least (Fig. 6*b*). This binding greatly increases with the removal of both GDP and GTP, with half-maximal receptor occupancy shifted towards lower [D] values by 2.6 to 3.1 logs.

As [D] increases, the GPCR coupling in the low-pre-coupling system always rises, from 0.05% to 9.5% (GTP only); from 1.7% to 13.4% (no GTPase activity); from 1.7% to 58.4%

(k_{GTP} = 0.25/s); from 1.9% to 76.8% (GDP only); and finally, from 88.4% to 100% (no GDP or GTP) (Fig. 6*c*).

High constitutive activity: To model the conditions of partial and inverse agonism, the standard system was simulated with the modification of "high constitutive activity" (where the receptor had isomerization constant K_q = 0.01; see Table I for parameters used for variable agonists). In the absence of agonist, activity is about tenfold greater than that of the standard system (Fig. 7*a*). Agonist-induced activity increases to a greater extent with the more efficacious agonist as compared to that observed for the partial agonist, whereas the inverse agonist inhibits activity. Fig. 7*b* shows the associated occupancy; the partial agonist binds more weakly than the efficacious by 1.5 to 1.6 logs due to weaker affinity for the active state of the receptor, while the inverse agonist binds more strongly than the efficacious by 0.8 log, due to overall higher affinity for the receptor, particularly its inactive state. Fig. 7*c* shows coupling according to agonist variety; only the efficacious agonist exhibits an increase in coupling with higher concentration (the other agonists have little concentration dependence). The transduced activity (K_E = 15 molecules) for the three kinds of agonists is shown in Fig. 7*d*, behaving very much as expected. At low concentration, all three agonists have a transduced activity (0.375) approximately equivalent to that caused by constitutive receptor activity. For high ligand concentrations, the activity approaches a limit of 0.98 for the efficacious agonist, 0.76 for the partial agonist and 0.06 for the inverse agonist.

To investigate partial agonism more closely, we modeled a second partial agonist for the standard case where the receptor has its usual low constitutive activity. This partial agonist has a K_b/K_a affinity constant ratio of 40, compared to 3333 for the efficacious agonist (see Table 2). Maximum induced activity is greater for the more efficacious agonist as compared to the rather small activating effect of the partial agonist (Fig. 8*a*). The partial agonist binds more weakly to the receptor than the efficacious by ¼ log (Fig. 8*b*) due to reduced affinity for the active state of the receptor. As in Fig. 7*c*, the efficacious agonist shows a slight increase in coupling at high

ligand concentration while the partial agonist's coupling profile is flat (Fig. 8*c*). The transduced activation is shown in Fig. 8*d* (K_E = 25 molecules), and is zero in the limit of low ligand concentration. At high agonist levels, the transduced activation tends to 0.286 for the partial agonist compared to 0.94 for the efficacious one.

The effects of guanine nucleotide on the system with high constitutive activity are shown in Fig. 9 for the efficacious agonist (Fig. 9*a–b*), partial agonist (Fig. 9*c–d*) and inverse agonist (Fig. 9*e–f*). As in most of the other systems, the occupancies are essentially equal when at least one type of guanine nucleotide present (Fig. 9*a*,*c*,*e*). When both GDP and GTP are removed, the ligand binding strengthens by almost 1½ logs for the efficacious agonist (Fig. 9*a*), by nearly ⅜ log for the partial agonist (Fig. 9*c*), and actually weakens by nearly ⅓ log for the inverse agonist (Fig. 9*e*). The efficacious agonist has a small effect on promoting GPCR coupling in the presence of both guanine nucleotides, and a slightly larger effect when only GDP is present (Fig. 9*b*), but the coupling is unchanged by either the partial or inverse agonist (Fig. 9*d*,*f*). Without either GDP or GTP, the GPCR pre-coupling rate of 58% is increased to 94% by the efficacious agonist (Fig. 9*b*) and to 75% by the partial agonist (Fig. 9*d*), while it is decreased to 32% by the inverse agonist (Fig. 9*f*). This last result is in line with the expected effects of inverse agonism, as the relatively large amount of pre-coupling in this case can be attributed to the high level of constitutive receptor activity.

Consistently low pre-coupling: In addition to the above, we modeled a system in which the pre-coupling is low, even in the absence of GDP and GTP. The parameters of this model involved adjusting the low pre-coupling system so that both K_q and K_p (the isomerization constants of the receptor and G protein respectively) were decreased by a factor of 10 and K_b increased by a factor of 6 to maintain substantial signaling activity. In the presence of both GDP and GTP, this system indeed exhibits a maximum agonist-induced activity of nearly 400 molecules (Fig. 10*a*). The agonist binding increases by about 2.8 logs in the absence of guanine nucleotide (Fig. 10*b*), roughly comparable to the effect for the same system but with high pre-coupling in the absence

of guanine nucleotide (Fig. 6*b*). The coupling profile (Fig. 10*c*) verifies that the pre-coupling of the GPCR is low (9.36%) in the absence of GDP or GTP. Interestingly, in this consistently low pre-coupling system, the coupling at high agonist concentration is lowered by removing GTP when both guanine nucleotides are present, in contrast to the similar system referenced in Fig. 6. A possible explanation for this phenomenon is that for high agonist concentration in the consistently low pre-coupling system, the coupling level of GPCRs to G_{GDP} increases from 23.3% to 31.1% when GTP is removed, a rise of 7.8%, while in the other low pre-coupling system, the coupling of GPCRs to G_{GDP} increases from 23.0% to 50.6%, for a rise of 27.6%. In addition, in the consistently low pre-coupling system, the coupling level of GPCRs to $G_{(no\ X)}$ increases from 3.1% to 5.4% when GTP is removed, a rise of 2.3%, and from 6.5% to 26.3% with regular low pre-coupling, for a rise of 19.8% (data not shown). Therefore, in the consistently low pre-coupling system, the removal of GTP fails to produce enough additional RG_{GDP} and RG to make up for the lost RG_{GTP}, in contrast to the other low pre-coupling system, where the additional RG_{GDP} and RG more than make up for the lost RG_{GTP}, even though there is more RG_{GTP} to replace in the latter system (29%, compared with 14% for consistently low pre-coupling).

Analysis of the transduced activity of agonists: We analyzed the simulated concentration-response curves of the agonists to estimate the K_b and relative K_b values (RA_i) for the data in Figs. 7*d* and 8*d*, respectively.

As described previously (20), when concentration-response curves exhibit constitutive activity, it is always possible to estimate the K_b value of orthosteric ligands in units of M^{-1}. Consequently, equation 4 was fitted to the simulated data in Figure 7*d* by global nonlinear regression analysis. This analysis yielded estimates of log K_b for the most efficacious agonist (7.74), partial agonist I (4.97), and the inverse agonist (5.54). These estimates are nearly the same as those used to simulate the data: efficacious agonist (7.70), partial agonist I (4.79) and inverse agonist (5.54) (see Table I). This analysis also yielded estimates of the log observed

affinity constant (log K_{obs}) of partial agonist I (4.22) and the inverse agonist (6.48). The latter values are nearly the same as the pEC_{50} values of these ligands for G protein activation: 4.22 and 6.51, respectively.

Global nonlinear regression analysis of the simulated full agonist and partial agonist concentration-response curves in Fig. 8*d* using equations 2 and 3, respectively, yielded an estimate of the log K_b value of partial agonist II relative to the more efficacious agonist (i.e., log RA_i, -1.95). This value is nearly the same as that used to simulate the data (-1.92). The analysis also yielded an estimate of the log K_{obs} of partial agonist II (4.12) and this estimate is nearly the same as the pEC_{50} value for G protein activation (4.14).

DISCUSSION

Our kinetic model has provided insight into the behavior of GPCR systems under various conditions, particularly with regard to G protein activity, receptor binding with ligand, and G protein-GPCR coupling. From the above results, we can confirm the intuitive hypotheses that G protein activity increases with a decrease in the rate of GTPase activity (Fig. 3) and that, in the presence of excess G protein, receptors can induce additional activity. Removing both GDP and GTP from the system dramatically increase both GPCR coupling and agonist binding, illustrating the negative cooperativity between the binding of guanine nucleotide and ligand to the G protein-GPCR complex. The inhibitory effects of guanine nucleotides on agonist affinity are proportional to ligand efficacy, and in the presence of constitutive activity, guanine nucleotides increase the affinity of inverse agonists while reducing the affinity of agonists. The latter effects have been reproduced in cell homogenates expressing G_i-linked GPCRs in the presence of low sodium, a condition that increases activation of the unoccupied receptor (22).

By itself, G protein activation (GTP binding to G protein) reduces the amount of GPCR coupling and contributes to the net effect of the agonist on coupling depending on GTPase activity, the availability of G protein and the amount of pre-coupling. For the standard system (limiting G protein and moderate receptor pre-coupling (23%) primarily due to the species RG_{GDP}), a maximally effective agonist concentration causes a small increase in GPCR coupling (3%), which is converted into a substantial reduction in coupling in the absence of GTPase activity (Fig. 3). Increasing the ratio of G protein to receptor greatly increases pre-coupling and gives rise to agonist-induced receptor decoupling, particularly in the absence of GTPase activity (Fig. 5). Coupling decreases with agonist concentration only in the presence of both GDP and GTP, a phenomenon that follows logically from the following properties of the system: 1) The pre-coupled receptor species is primarily RG_{GDP}, 2) agonist-induced G protein activation involves GTP/GDP exchange, and 3) the resulting GTP-bound G proteins are unavailable for

GPCR coupling. In contrast, when GPCR coupling is low, agonist-induced receptor activation causes an increase in coupling (Figs. 6 and 10).

One unexpected finding is that in systems with a high G protein to receptor ratio, adding agonist causes activity to fall slightly in the presence of GTP without GDP. This is likely to be related to the negative cooperativity phenomenon noted above as agonist binding causes a decrease in G protein binding to GTP. Nonetheless, the addition of agonist greatly accelerates the attainment of steady state activity for this condition (data not shown).

Our results have implications with regard to experiments utilizing BRET or FRET probes attached to the receptor and G protein to monitor their coupling as described under "Introduction". We show that substantial pre-coupling can occur in the absence of constitutive receptor activity and that agonist-induced receptor activation can occur with little change, or an increase or decrease in GPCR coupling under this condition. Substantial agonist-induced receptor coupling can also occur without much pre-coupling. Thus, our results can explain agonist-induced increases or decrease in resonance energy transfer between fluorescent or luminescent and fluorescent proteins attached to receptor and G protein that are associated with the corresponding changes in coupling. Of course, agonist-induced conformational changes in the receptor and G protein can lead to resonance energy transfer independently of changes in coupling as explained by Audet and coworkers (17) in their studies on the α_{2A} receptor. The question remains as to what extent the G protein class, the GPCR and the nature of the receptor scaffold determine the extent of receptor pre-coupling and the nature of the agonist-induced changes in coupling. We find that the most optimal condition for agonist-induced G protein activation occurs with a high ratio of G protein to receptor and a high pre-coupling of the inactive state of the GDP-bound G protein to the inactive state of the receptor (RG_{GDP}). To what extent this condition exists in nature is unclear. There is evidence that the M_3 muscarinic receptors exhibit low pre-coupling (23), whereas α_{2A} receptors exhibit substantial pre-coupling (16).

In the present study, we chose to simulate the condition where G protein activation is associated with dissociation of the holoprotein into $G\alpha_{GTP}$ and $G\beta\gamma$ subunits. Studies using BRET probes on agonist-induced activation of $G\alpha_{i1}$ strongly suggest a lack of dissociation of the holoprotein with activation. Our model can be modified to account for this condition by defining an affinity constant for the equilibrium between $G\alpha_{GTP}$ and $G\beta\gamma$ such that these are primarily in the holoprotein form at steady state. One possibility is that although individual subunits may be in the holoprotein complex at steady state, this complex could be readily reversible such that the individual $G\alpha_{GTP}$ and $G\beta\gamma$ subunits can dissociate and form high affinity complexes with their respective effectors. This postulate is consistent with the observation that a stable GTP-bound holoprotein complex does not survive biochemical isolation and that crystal structures of GTPγS bound $G\alpha_i$ have been solved (24) but not of the GTPγS-bound holoprotein. Of course, the structure of the GDP-bound holoprotein has been solved (25).

We have also used the steady state model to simulate downstream agonist concentration-response curves. This has enabled the validation of our approach for estimating relative (RA_i) and absolute (K_b) estimates of orthosteric ligand affinity constants for the active receptor state. As described previously (26), it is always possible to obtain an estimate of the affinity constant of an agonist for the active receptor state expressed relative to that of a standard agonist even if there is insufficient information to estimate the product of affinity and efficacy of either agonist. This relationship occurs because the active state affinity constant is an independent parameter that determines the population constants of affinity and efficacy (6, 20). Whenever a receptor signaling pathway exhibits constitutive activity, it is also possible to estimate the active state affinity constant in absolute units of M^{-1} (20). The present results also validate the estimation of this parameter. Finally, our results also illustrate that the observed dissociation constant of the orthosteric ligand is equivalent to the concentration of agonist required for half maximal G protein activation. This result is generally constituent with prior work illustrating that the observed dissociation constant is equivalent to the EC_{50} value of ligand required for half-

maximal changes in the amount of quaternary complex consisting of ligand, the active state of the receptor and GDP-bound G protein (3, 4, 27).

CONCLUSIONS

Our results show optimal G protein activation with substantial receptor-G protein precoupling and that agonist-induced G protein activation can occur with increases, decreases or no change in G protein coupling. These results have direct implications to the analysis of receptor-G protein interactions using FRET and BRET. In addition we have validated our prior methods for quantifying agonist bias through estimation of relative and absolute active state affinity constants.

DECLARATIONS OF INTEREST

The authors report no declarations of interest.

APPENDIX

This Appendix briefly describes how microscopic reversibility was maintained throughout our model (Fig. 1). In addition a series of tables listing the rate constants used in the model are introduced below.

The process of maintaining microscopic reversibility with regard to the assignment of affinity and isomerization constants is illustrated in relation to the square of equilibria shown in Fig. 11. First, the simple equilibrium constants (K_a, K_b and K_q) are assigned to their respective equilibria, based on the definitions described in Table 1. Next, the two possible routes from the simplest receptor species (R, origin) to the most complex (DR*, destination) are identified. The first involves the route from R to R* to DR* (route 1) and the second from R to DR to DR* (route 2). Then an equilibrium route parameter is defined for each of the two equilibrium steps in a route. If the step involves forming a bound complex or isomerization from resting to active or exchange states, then the equilibrium route parameter is equivalent to the corresponding affinity constant or isomerization constant. In contrast, if the route involves the dissociation of a complex or the isomerization to the inactive state, then the equilibrium route parameter is equivalent to the reciprocal of the corresponding affinity constant or isomerization constant. Next, the product of the two equilibrium route parameters for each route is determined. These products are K_qK_b (route 1) and K_ax (route 2), where x denotes the unknown equilibrium route parameter for the step from DR to DR*. These two products are equivalent ($K_qK_b = K_ax$), so it follows that $x = K_bK_q/K_a$. Finally, if x defines the formation of a bound complex or isomerization into an active state, then the equilibrium parameter for the step is equivalent to x. Otherwise, the equilibrium parameter is equivalent to 1/x.

This general strategy is used to define all of the equilibria in Fig. 1 by using constants defined in Table 1 as well as previously determined constants (e.g., K_bK_q/K_a for the transition from DR to DR*). It is unnecessary to identify routes from the simplest to the most complex species in a given square or to identify two routes of equal length. For example, the three step

route from DR to R to R* to DR* yields three equilibrium route parameters of $1/K_a$, K_q and K_b. Their product (K_bK_q/K_a) is equivalent to the equilibrium route parameter for the alternative route from DR to DR* (x).

The values for the various rate constants used for the model (Fig.1) are given in Tables 3–7. The Tables include the rate constants for guanine nucleotide binding (Table 3), receptor-G protein interactions (Table 4), receptor and G protein isomerization (Table 5), ligand binding to receptor (Table 6) and processes involving the dissociated form of the G protein (Table 7).

REFERENCES

1 DeWire SM, Ahn S, Lefkowitz RJ, Shenoy SK. Beta-arrestins and cell signaling. Annu Rev Physiol. 2007;69:483-510.

2 Lefkowitz RJ. A brief history of G-protein coupled receptors (Nobel Lecture). Angew Chem Int Ed Engl. 2013 Jun 17;52(25):6366-78.

3 Ehlert FJ, Rathbun BE. Signaling through the muscarinic receptor-adenylate cyclase system of the heart is buffered against GTP over a range of concentrations. Mol Pharmacol. 1990;38(1):148-58.

4 Ehlert FJ. Ternary Complex Model. In: Christopoulos A, ed. *Biomedical Applications of Computer Modeling*. Boca Raton: CRC Press 2000:21-85.

5 Tran JA, Chang A, Matsui M, Ehlert FJ. Estimation of relative microscopic affinity constants of agonists for the active state of the receptor in functional studies on M_2 and M_3 muscarinic receptors. Mol Pharmacol. 2009 Feb;75(2):381-96.

6 Ehlert FJ, Griffin MT. Estimation of ligand affinity constants for receptor states in functional studies involving the allosteric modulation of G protein-coupled receptors: implications for ligand bias. J Pharmacol Toxicol Methods. 2014 May-Jun;69(3):253-79.

7 Berrie CP, Birdsall NJ, Burgen AS, Hulme EC. Guanine nucleotides modulate muscarinic receptor binding in the heart. Biochem Biophys Res Comm. 1979;87(4):1000-5.

8 Childers SR, Snyder SH. Guanine nucleotides differentiate agonist and antagonist interactions with opiate receptors. Life Sci. 1978;23:759-62.

9 Freedman SB, Poat JA, Woodruff GN. Effect of guanine nucleotides on dopaminergic agonist and antagonist affinity for [3H]sulpiride binding sites in rat striatal membrane preparations. J Neurochem. 1981 Sep;37(3):608-12.

10 Waelbroeck M, Boufrahi L, Swillens P. Seven Helix Receptors are Enzymes Catalysing G Protein Activation. What is the Agonist Kact? J Theor Biol. 1997;187(1):15-37.

11 Shea LD, Neubig RR, Linderman JJ. Timing is everything the role of kinetics in G protein activation. Life Sci. 2000 Dec 29;68(6):647-58.

12 Heitzler D, Durand G, Gallay N, Rizk A, Seungkirl Ahn S, Kim J, et al. Competing G protein-coupled receptor kinases balance G protein and β-arrestin signaling. Molecular Systems Biology. 2012;8:590.

13 Vayttaden SJ, Friedman J, Tran TM, Rich TC, Dessauer CW, Clark RB. Quantitative modeling of GRK-mediated beta2AR regulation. PLoS Comput Biol. 2010 Jan;6(1):e1000647.

14 Hein P, Frank M, Hoffmann C, Lohse MJ, Bunemann M. Dynamics of receptor/G protein coupling in living cells. Embo J. 2005 Dec 7;24(23):4106-14.

15 Hein P, Rochais F, Hoffmann C, Dorsch S, Nikolaev VO, Engelhardt S, et al. Gs activation is time-limiting in initiating receptor-mediated signaling. J Biol Chem. 2006 Nov 3;281(44):33345-51.

16 Gales C, Van Durm JJ, Schaak S, Pontier S, Percherancier Y, Audet M, et al. Probing the activation-promoted structural rearrangements in preassembled receptor-G protein complexes. Nat Struct Mol Biol. 2006 Sep;13(9):778-86.

17 Audet N, Gales C, Archer-Lahlou E, Vallieres M, Schiller PW, Bouvier M, et al. Bioluminescence resonance energy transfer assays reveal ligand-specific conformational changes within preformed signaling complexes containing delta-opioid receptors and heterotrimeric G proteins. J Biol Chem. 2008 May 30;283(22):15078-88.

18 Traut TW. Physiological concentrations of purines and pyrimidines. Mol Cell Biochem. 1994 Nov 9;140(1):1-22.

19 Black JW, Leff P. Operational models of pharmacological agonism. Proceedings of the Royal Society of London Series B: Biological Sciences. 1983;220(1219):141-62.

20 Ehlert FJ, Suga H, Griffin MT. Analysis of agonism and inverse agonism in functional assays with constitutive activity: estimation of orthosteric ligand affinity constants for active and inactive receptor states. J Pharmacol Exp Ther. 2011 Aug;338(2):671-86.

21 Ehlert FJ, Suga H, Griffin MT. Quantifying agonist activity at G protein-coupled receptors. J Vis Exp. 2011(58):e3179.

22 Hulme EC, Berrie CP, Birdsall NJ, Burgen AS. Two populations of binding sites for muscarinic antagonists in the rat heart. Eur J Pharmacol. 1981;73(2-3):137-42.

23 Zurn A, Zabel U, Vilardaga JP, Schindelin H, Lohse MJ, Hoffmann C. Fluorescence resonance energy transfer analysis of alpha 2a-adrenergic receptor activation reveals distinct agonist-specific conformational changes. Mol Pharmacol. 2009 Mar;75(3):534-41.

24 Coleman DE, Berghuis AM, Lee E, Linder ME, Gilman AG, Sprang SR. Structures of active conformations of Gi alpha 1 and the mechanism of GTP hydrolysis. Science. 1994 Sep 2;265(5177):1405-12.

25 Wall MA, Coleman DE, Lee E, Iniguez-Lluhi JA, Posner BA, Gilman AG, et al. The structure of the G protein heterotrimer Gi alpha 1 beta 1 gamma 2. Cell. 1995 Dec 15;83(6):1047-58.

26 Griffin MT, Figueroa KW, Liller S, Ehlert FJ. Estimation of Agonist Activity at G Protein-Coupled Receptors: Analysis of M2 Muscarinic Receptor Signaling through Gi/o,Gs, and G15. J Pharmacol Exp Ther. 2007 Jun;321(3):1193-207.

27 Ehlert FJ. On the analysis of ligand directed signaling at G protein coupled receptors. NS Arch Pharmacol. 2008;377:549-77.

Figure Legends

Figure 1. Possible binding complexes in the GPCR quaternary complex model. (a) The model shows the various complexes for the interaction between a receptor that exists in active (R*) and inactive (R) states and the inactive (G) and exchange (G*) states of the holoprotein form of the G protein. The binding reactions of ligand (D) to the receptor and of the guanine nucleotides, GTP and GDP, to the G protein are also shown. (b) The various steps involved in the dissociation of the GTP-bound form of the G protein into its active Gα (Gα**) and Gβγ subunits and their ultimate conversion into GDP-bound form of the G protein.

Figure 2. Time-dependent approach to equilibrium in the absence of agonist when all G protein in the model is initially complexed with either GDP or GTP. Properties shown are activity (a) and GPCR coupling (b).

Figure 3. Simulation of agonist dependence in the standard system. Properties shown are activity (a), occupancy (b), coupling (c) and transduced activity (d). Activity is defined as the number of G protein molecules in the state $G^{**}\alpha_{GTP} + G\beta\gamma$. The parameter values $K_E = 50$ molecules and $m = 1$ were used to transduce the activity (equation 1).

Figure 4. Simulation of the effects of guanine nucleotide on agonist-dependent properties in the standard system. Properties shown are activity (a), occupancy (b) and coupling (c).

Figure 5. Simulation of the effects of excess G protein (5.6234:1 ratio with GPCR) on agonist dependence. Properties shown are activity (a), occupancy (b) and coupling (c).

Figure 6. Simulation of the effects of excess G protein and low pre-coupling conditions on agonist dependence. Properties shown are activity (a), occupancy (b) and coupling (c).

Figure 7. Simulation of the effects of efficacious, partial and inverse agonism on a system with high constitutive receptor activity ($K_q = 10^{-2}$). Properties shown are transduced activity (a), occupancy (b), coupling (c) and standard molecular activity (d), defined as the number of G protein molecules in the state $G^{**}\alpha_{GTP} + G\beta\gamma$. The parameter values $K_E = 15$ molecules and $s = 1$ were used to transduce the activity.

Figure 8. Simulation of the effects of efficacious and partial agonism on the standard system with low constitutive activity ($K_q = 2 \times 10^{-4}$). Properties shown are standard molecular activity, defined as the number of G protein molecules in the state $G^{**}\alpha_{GTP} + G\beta\gamma$ (a), occupancy (b), coupling (c) and transduced activity (d). The parameter values $K_E = 25$ molecules and $m = 1$ were used to transduce the activity (equation 1).

Figure 9. Simulation of the effects of guanine nucleotide and efficacious, partial and inverse agonism on occupancy and coupling in the system with high constitutive activity. Properties shown are occupancy (a,c,e) and coupling (b,d,f) in the cases of efficacious agonist (a–b), partial agonist (c–d) and inverse agonist (e–f).

Figure 10. Simulation of the effects of conditions in which pre-coupling is low even in the absence of both GDP and GTP ($K_q = 2 \times 10^{-5}$; $K_p = 10^{-5}$; $K_b/K_a = 2 \times 10^{4}$). Properties shown are activity (a), occupancy (b) and coupling (c).

Figure 11. Example of the preservation of microscopic reversibility. The illustration shows how to estimate the isomerization constant for the occupied receptor from the more fundamental constants describing the isomerization of the unoccupied receptor (K_q) and ligand affinity for the

active (K_b) and inactive (K_a) states of the receptor. The two different routes from the simplest receptor species (R) to the most complex (DR*) are shown.

TABLE 1. Equilibrium constants used in the kinetic model.

Include all agonists

Constant	Reaction	Value
$\mathbf{K_a}$	D + R ⇆ DR	1.5 x 10^4 M^{-1} (efficacious agonist) 1.5 x 10^4 M^{-1} (partial agonists I and II) 3.5 x 10^6 M^{-1} (inverse agonist)
$\mathbf{K_b}$	D + R* ⇆ DR*	5 x 10^7 M^{-1} (efficacious agonist) 6 x 10^4 M^{-1} (partial agonist I) 6 x 10^5 M^{-1} (partial agonist II) 3.5 x 10^5 M^{-1} (inverse agonist)
$\mathbf{K_i}$	R + G ⇆ RG	4 x 10^{-5} M^{-1} (high-pre-coupling system) 1.6 x 10^{-7} M^{-1} (low-pre-coupling system)
$\mathbf{K_j}$	R* + G ⇆ R*G	7.5 x 10^{-5} M^{-1} (high-pre-coupling system) 1.25 x 10^{-5} M^{-1} (low-pre-coupling system)
$\mathbf{K_k}$	R* + G* ⇆ R*G*	3 x 10^2 M^{-1} (high-pre-coupling system) 4.5 x 10^3 M^{-1} (low-pre-coupling system)
$\mathbf{K_q}$	R ⇆ R*	2 x 10^{-4} (low constitutive activity) 10^{-2} (high constitutive activity)
$\mathbf{K_p}$	G ⇆ G*	10^{-4}
$\mathbf{K_v}$	G + GTP ⇆ G_{GTP}	10^5 M^{-1}
$\mathbf{K_x}$	G + GDP ⇆ G_{GDP}	10^8 M^{-1}
$\mathbf{K_y}$	G* + X ⇆ G^*_X, where X = GTP or GDP	10^4 M^{-1}
$\mathbf{K_{act}}$	G_{GTP} or G^*_{GTP} ⇆ G**α_{GTP} + Gβγ	4.64 M

Change table; identify standard system, denote differences from it. Only two headings on left: Standard system and changes from

TABLE 2. Systems simulated in the kinetic model.

System Conditions	Changes from Standard System
Standard system	~~N/A~~ see Tables 3-7
High RGS activity	k_{GTP} = 0.8/s
Low RGS activity	k_{GTP} = 0.125/s
No GTPase activity	k_{GTP} = 0
No X	[GDP] = [GTP] = 0
No GTP	[GDP] normal, [GTP] = 0
No GDP	[GDP] = 0, [GTP] normal (non-hydrolyzable)
High ratio	"High G/R" (# of G protein molecules = 56,234)
High ratio, no GTPase activity	High G/R, k_{GTP} = 0
High ratio, no X	High G/R, [GDP] = [GTP] = 0
High ratio, no GTP	High G/R, [GTP] = 0
High ratio, no GDP	High G/R, [GDP] = 0
Low-pre-coupling system	High G/R, "low pre-coupling" (K_i, K_j and K_k set to low-pre-coupling system values; see Table I)
Low-pre-coupling, no GTPase activity	High G/R, low pre-coupling, k_{GTP} = 0
Low-pre-coupling, no X	High G/R, low pre-coupling, [GDP] = [GTP] = 0
Low-pre-coupling, no GTP	High G/R, low pre-coupling, [GTP] = 0
Low-pre-coupling, no GDP	High G/R, low pre-coupling, [GDP] = 0
High constitutive activity	$K_q = 10^{-2}$

TABLE 3. Rate constants for guanine nucleotide association/dissociation.

Reaction	Rate ~~Constant Value~~
$G_{GDP} \rightarrow G + GDP$	10^{-4} s^{-1}
$G + GDP \rightarrow G_{GDP}$	10^{4} M^{-1} s^{-1}
$G + GTP \rightarrow G_{GTP}$	10^{4} M^{-1} s^{-1}
$G_{GTP} \rightarrow G + GTP$	0.1 s^{-1}
$RG_{GDP} \rightarrow RG + GDP$	10^{-4} s^{-1}
$RG + GDP \rightarrow RG_{GDP}$	10^{4} M^{-1} s^{-1}
$RG + GTP \rightarrow RG_{GTP}$	10^{4} M^{-1} s^{-1}
$RG_{GTP} \rightarrow RG + G_{GTP}$	0.1 s^{-1}
$R^*G_{GDP} \rightarrow R^*G + GDP$	10^{-4} s^{-1}
$R^*G + GDP \rightarrow R^*G_{GDP}$	10^{4} M^{-1} s^{-1}
$R^*G + GTP \rightarrow R^*G_{GTP}$	10^{4} M^{-1} s^{-1}
$R^*G_{GTP} \rightarrow R^*G + G_{GTP}$	0.1 s^{-1}
$G^*_{GDP} \rightarrow G^* + GDP$	100 s^{-1}
$G^* + GDP \rightarrow G^*_{GDP}$	10^{6} M^{-1} s^{-1}
$G^* + GTP \rightarrow G^*_{GTP}$	10^{6} M^{-1} s^{-1}
$G^*_{GTP} \rightarrow G^* + GTP$	100 s^{-1}
$R^*G^*_{GDP} \rightarrow R^*G^* + GDP$	100 s^{-1}
$R^*G^* + GDP \rightarrow R^*G^*_{GDP}$	10^{6} M^{-1} s^{-1}
$R^*G^* + GTP \rightarrow R^*G^*_{GTP}$	10^{6} M^{-1} s^{-1}
$R^*G^*_{GTP} \rightarrow R^*G^* + GTP$	100 s^{-1}
$DRG_{GDP} \rightarrow DRG + GDP$	10^{-4} s^{-1}
$DRG + GDP \rightarrow DRG_{GDP}$	10^{4} M^{-1} s^{-1}
$DRG + GTP \rightarrow DRG_{GTP}$	10^{4} M^{-1} s^{-1}
$DRG_{GTP} \rightarrow DRG + G_{GTP}$	0.1 s^{-1}
$DR^*G_{GDP} \rightarrow DR^*G + GDP$	10^{-4} s^{-1}
$DR^*G + GDP \rightarrow DR^*G_{GDP}$	10^{4} M^{-1} s^{-1}
$DR^*G + GTP \rightarrow DR^*G_{GTP}$	10^{4} M^{-1} s^{-1}
$DR^*G_{GTP} \rightarrow DR^*G + G_{GTP}$	0.1 s^{-1}
$DR^*G^*_{GDP} \rightarrow DR^*G^* + GDP$	100 s^{-1}
$DR^*G^* + GDP \rightarrow DR^*G^*_{GDP}$	10^{6} M^{-1} s^{-1}
$DR^*G^* + GTP \rightarrow DR^*G^*_{GTP}$	10^{6} M^{-1} s^{-1}
$DR^*G^*_{GTP} \rightarrow DR^*G^* + GTP$	100 s^{-1}

TABLE 4. Rate constants for G protein–receptor coupling/decoupling.

In these reactions, the concentration of G protein is expressed relative to receptor

Reaction	Rate Constant Value
$R + G_{GDP} \rightarrow RG_{GDP}$	3×10^{-6} (#/cell)$^{-1}$ s^{-1}
$RG_{GDP} \rightarrow R + G_{GDP}$	0.075 s^{-1}
$R + G \rightarrow RG$	3×10^{-6} (#/cell)$^{-1}$ s^{-1}
$RG \rightarrow R + G$	0.075 s^{-1}
$R + G_{GTP} \rightarrow RG_{GTP}$	3×10^{-6} (#/cell)$^{-1}$ s^{-1}
$RG_{GTP} \rightarrow R + G_{GTP}$	0.075 s^{-1}
$R^* + G_{GDP} \rightarrow R^*G_{GDP}$	10^{-3} (#/cell)$^{-1}$ s^{-1}
$R^*G_{GDP} \rightarrow R^* + G_{GDP}$	13.3333 s^{-1}
$R^* + G \rightarrow R^*G$	10^{-3} (#/cell)$^{-1}$ s^{-1}
$R^*G \rightarrow R^* + G$	13.3333 s^{-1}
$R^* + G_{GTP} \rightarrow R^*G_{GTP}$	10^{-3} (#/cell)$^{-1}$ s^{-1}
$R^*G_{GTP} \rightarrow R^* + G_{GTP}$	13.3333 s^{-1}
$R^* + G^*_{GDP} \rightarrow R^*G^*_{GDP}$	8×10^{-4} (#/cell)$^{-1}$ s^{-1}
$R^*G^*_{GDP} \rightarrow R^* + G^*_{GDP}$	2.66667×10^{-6} s^{-1}
$R^* + G^* \rightarrow R^*G^*$	8×10^{-4} (#/cell)$^{-1}$ s^{-1}
$R^*G^* \rightarrow R^* + G^*$	2.66667×10^{-6} s^{-1}
$R^* + G^*_{GTP} \rightarrow R^*G^*_{GTP}$	320 (#/cell)$^{-1}$ s^{-1}
$R^*G^*_{GTP} \rightarrow R^* + G^*_{GTP}$	1.06667 s^{-1}
$DR + G_{GDP} \rightarrow DRG_{GDP}$	3×10^{-6} (#/cell)$^{-1}$ s^{-1}
$DRG_{GDP} \rightarrow DR + G_{GDP}$	0.075 s^{-1}
$DR + G \rightarrow DRG$	3×10^{-6} (#/cell)$^{-1}$ s^{-1}
$DRG \rightarrow DR + G$	0.075 s^{-1}
$DR + G_{GTP} \rightarrow DRG_{GTP}$	3×10^{-6} (#/cell)$^{-1}$ s^{-1}
$DRG_{GTP} \rightarrow DR + G_{GTP}$	0.075 s^{-1}
$DR^* + G_{GDP} \rightarrow DR^*G_{GDP}$	10^{-3} (#/cell)$^{-1}$ s^{-1}
$DR^*G_{GDP} \rightarrow DR^* + G_{GDP}$	13.3333 s^{-1}
$DR^* + G \rightarrow DR^*G$	10^{-3} (#/cell)$^{-1}$ s^{-1}
$DR^*G \rightarrow DR^* + G$	13.3333 s^{-1}
$DR^* + G_{GTP} \rightarrow DR^*G_{GTP}$	10^{-3} (#/cell)$^{-1}$ s^{-1}
$DR^*G_{GTP} \rightarrow DR^* + G_{GTP}$	13.3333 s^{-1}
$DR^* + G^*_{GDP} \rightarrow DR^*G^*_{GDP}$	8×10^{-4} (#/cell)$^{-1}$ s^{-1}
$DR^*G^*_{GDP} \rightarrow DR^* + G^*_{GDP}$	2.66667×10^{-6} s^{-1}
$DR^* + G^* \rightarrow DR^*G^*$	8×10^{-4} (#/cell)$^{-1}$ s^{-1}
$DR^*G^* \rightarrow DR^* + G^*$	2.66667×10^{-6} s^{-1}
$DR^* + G^*_{GTP} \rightarrow DR^*G^*_{GTP}$	320 (#/cell)$^{-1}$ s^{-1}
$DR^*G^*_{GTP} \rightarrow DR^* + G^*_{GTP}$	1.06667 s^{-1}

TABLE 5. Rate constants for receptor / G protein isomerization.

Reaction	Rate Constant Value
R → R*	1 s^{-1}
R* → R	5000 s^{-1}
G_{GDP} → G^*_{GDP}	0.1 s^{-1}
G^*_{GDP} → G_{GDP}	10^7 s^{-1}
G → G*	0.1 s^{-1}
G* → G	1000 s^{-1}
G_{GTP} → G^*_{GTP}	0.1 s^{-1}
G^*_{GTP} → G_{GTP}	10^4 s^{-1}
RG_{GDP} → R^*G_{GDP}	1 s^{-1}
R^*G_{GDP} → RG_{GDP}	2666.67 s^{-1}
R^*G_{GDP} → $R^*G^*_{GDP}$	0.1 s^{-1}
$R^*G^*_{GDP}$ → R^*G_{GDP}	2.5 s^{-1}
RG → R*G	1 s^{-1}
R*G → RG	2666.67 s^{-1}
R*G → R*G*	0.1 s^{-1}
R*G* → R*G	2.5 x 10^{-4} s^{-1}
RG_{GTP} → R^*G_{GTP}	1 s^{-1}
R^*G_{GTP} → RG_{GTP}	2666.67 s^{-1}
R^*G_{GTP} → $R^*G^*_{GTP}$	0.1 s^{-1}
$R^*G^*_{GTP}$ → R^*G_{GTP}	2.5 x 10^{-3} s^{-1}
DR → DR*	7 s^{-1}
DR* → DR	10.5 s^{-1}
DRG_{GDP} → DR^*G_{GDP}	7 s^{-1}
DR^*G_{GDP} → DRG_{GDP}	5.6 s^{-1}
DR^*G_{GDP} → $DR^*G^*_{GDP}$	0.2 s^{-1}
$DR^*G^*_{GDP}$ → DR^*G_{GDP}	5 s^{-1}
DRG → DR*G	7 s^{-1}
DR*G → DRG	5.6 s^{-1}
DR*G → DR*G*	0.2 s^{-1}
DR*G* → DR*G	5 x 10^{-4} s^{-1}
DRG_{GTP} → DR^*G_{GTP}	7 s^{-1}
DR^*G_{GTP} → DRG_{GTP}	5.6 s^{-1}
DR^*G_{GTP} → $DR^*G^*_{GTP}$	0.2 s^{-1}
$DR^*G^*_{GTP}$ → DR^*G_{GTP}	5 x 10^{-3} s^{-1}

TABLE 6. Rate constants for ligand association/dissociation with GPCR.

Reaction	Rate Constant Value
D + R → DR	[D] · 10^5 M^{-1} s^{-1}
DR → D + R	6.66667 s^{-1}
D + RG_{GDP} → DRG_{GDP}	[D] · 10^5 M^{-1} s^{-1}
DRG_{GDP} → D + RG_{GDP}	6.66667 s^{-1}
D + RG → DRG	[D] · 10^5 M^{-1} s^{-1}
DRG → D + RG	6.66667 s^{-1}
D + RG_{GTP} → DRG_{GTP}	[D] · 10^5 M^{-1} s^{-1}
DRG_{GTP} → D + RG_{GTP}	6.66667 s^{-1}
D + R* → DR*	[D] · 10^5 M^{-1} s^{-1}
DR* → D + R*	2 x 10^{-3} s^{-1}
D + R*G_{GDP} → DR*G_{GDP}	[D] · 10^5 M^{-1} s^{-1}
DR*G_{GDP} → D + R*G_{GDP}	2 x 10^{-3} s^{-1}
D + R*G → DR*G	[D] · 10^5 M^{-1} s^{-1}
DR*G → D + R*G	2 x 10^{-3} s^{-1}
D + R*G_{GTP} → DR*G_{GTP}	[D] · 10^5 M^{-1} s^{-1}
DR*G_{GTP} → D + R*G_{GTP}	2 x 10^{-3} s^{-1}
D + R*G*$_{GDP}$ → DR*G*$_{GDP}$	[D] · 10^5 M^{-1} s^{-1}
DR*G*$_{GDP}$ → D + R*G*$_{GDP}$	2 x 10^{-3} s^{-1}
D + R*G* → DR*G*	[D] · 10^5 M^{-1} s^{-1}
DR*G* → D + R*G*	2 x 10^{-3} s^{-1}
D + R*G*$_{GTP}$ → DR*G*$_{GTP}$	[D] · 10^5 M^{-1} s^{-1}
DR*G*$_{GTP}$ → D + R*G*$_{GTP}$	2 x 10^{-3} s^{-1}

TABLE 7. Rate constants for processes involving G protein in dissociated form ($\alpha + \beta\gamma$).

Reaction	Rate Constant Value
$G^{**}\alpha_{GTP} \rightarrow G^{**}\alpha_{GDP}$	0.25 s^{-1}
$G_{GTP} \rightarrow G^{**}\alpha_{GTP} + G\beta\gamma$	2.924 s^{-1}
$G^{*}_{GTP} \rightarrow G^{**}\alpha_{GTP} + G\beta\gamma$	2.924 s^{-1}
$G^{**}\alpha_{GTP} + G\beta\gamma \rightarrow G_{GTP}$	0.63 s^{-1}
$G^{**}\alpha_{GTP} + G\beta\gamma \rightarrow G^{*}_{GTP}$	0.63 s^{-1}
$G^{**}\alpha_{GDP} \rightarrow G\alpha_{GDP}$	6×10^{-3} s^{-1}
$G\alpha_{GDP} \rightarrow G^{**}\alpha_{GDP}$	2.5×10^{-6} s^{-1}
$G\alpha_{GDP} + G\beta\gamma \rightarrow G_{GDP}$	6×10^{-3} s^{-1}

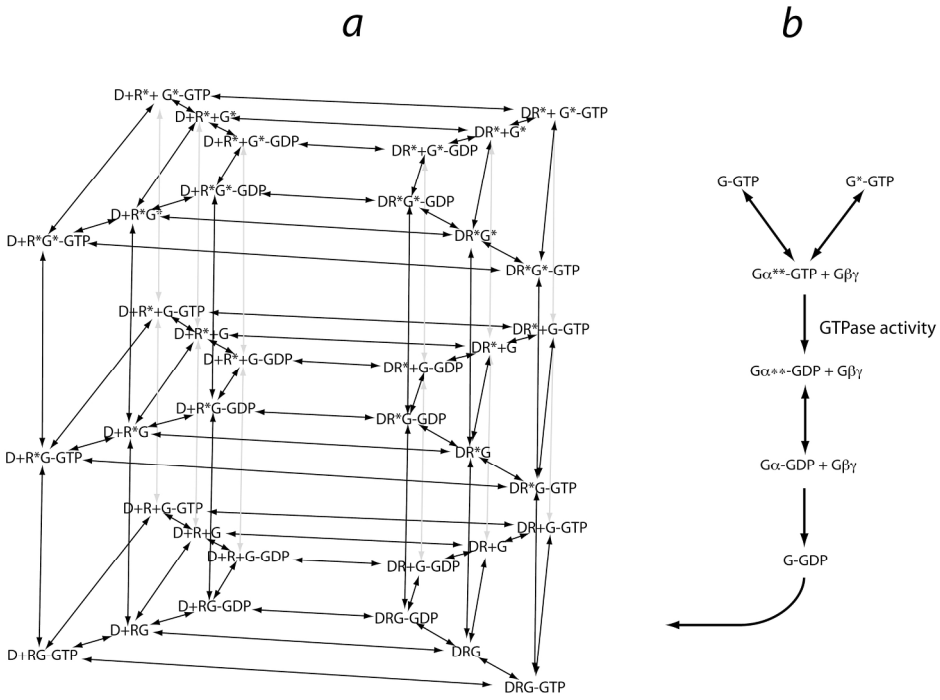

Figure 1
222x168mm (300 x 300 DPI)

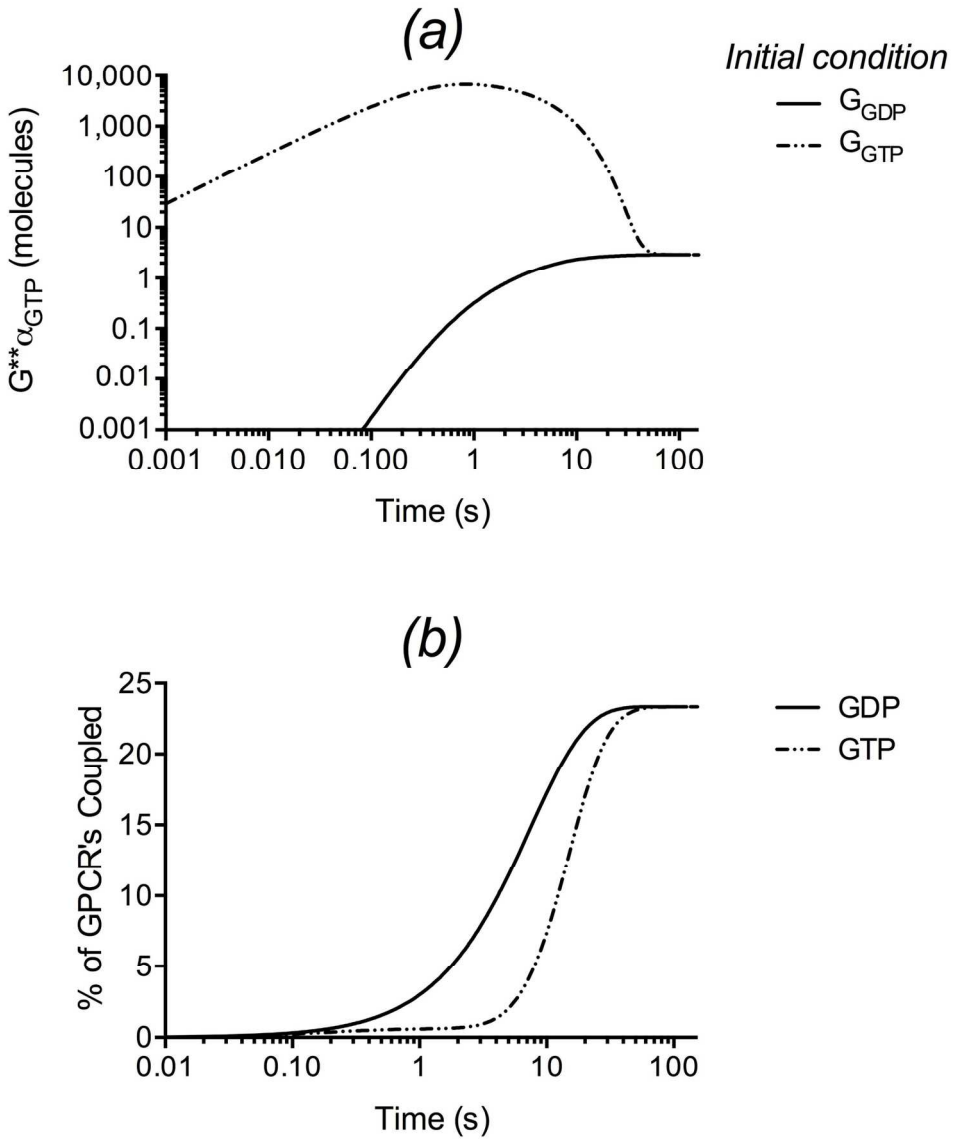

Figure 2
151x180mm (300 x 300 DPI)

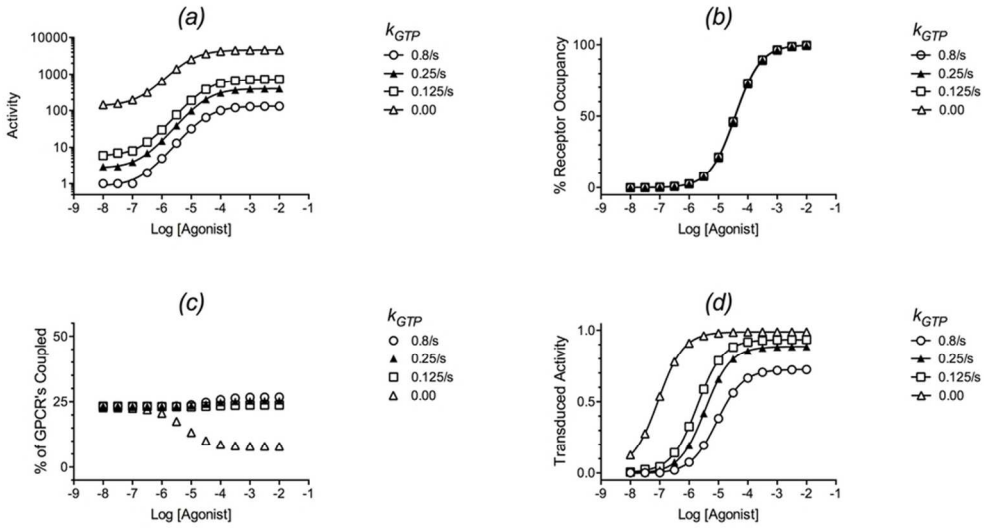

Figure 3
83x45mm (300 x 300 DPI)

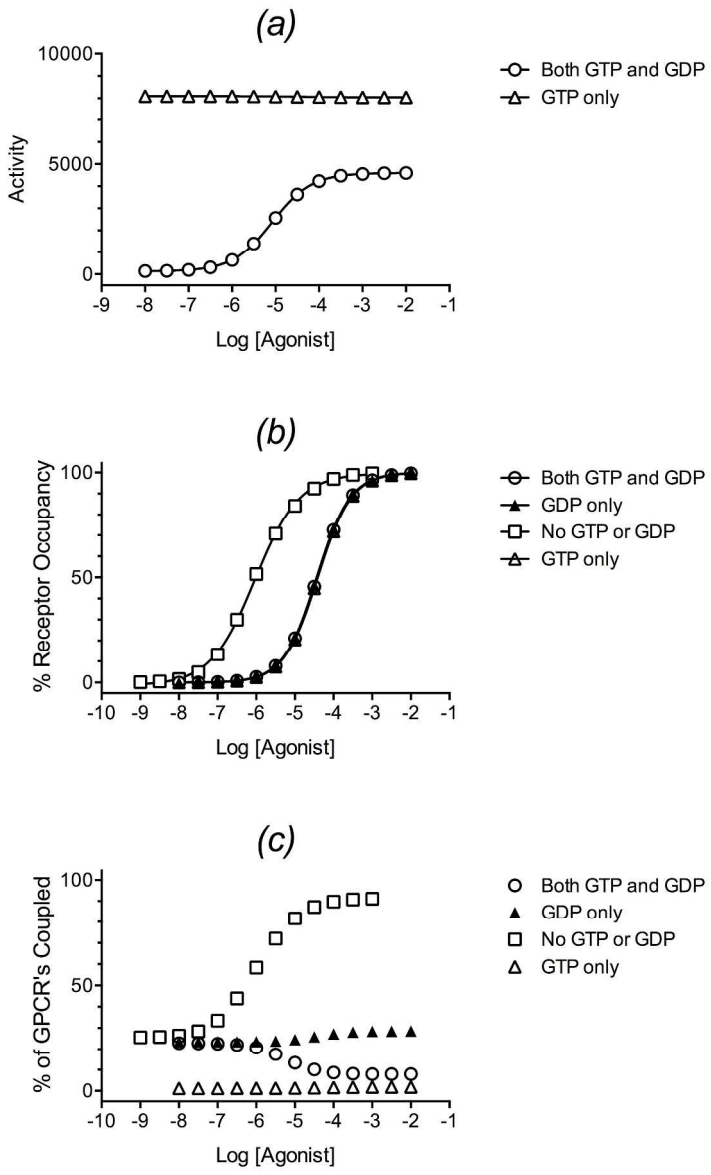

Figure 4
227x369mm (300 x 300 DPI)

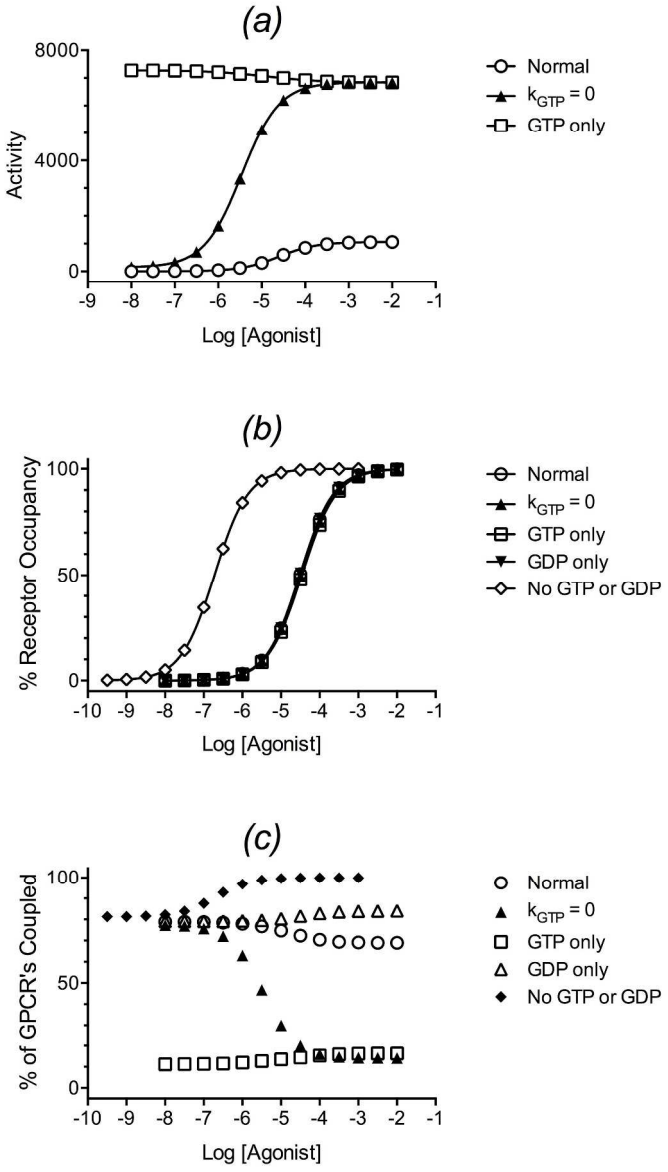

Figure 5
227x392mm (300 x 300 DPI)

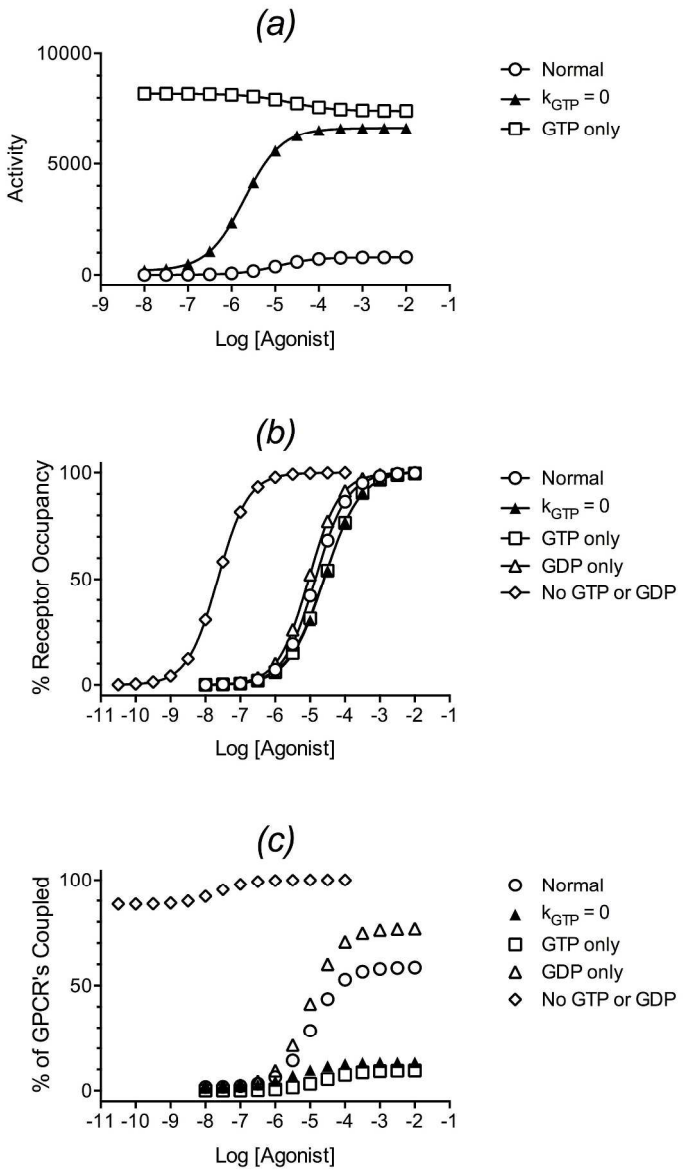

Figure 6
227x383mm (300 x 300 DPI)

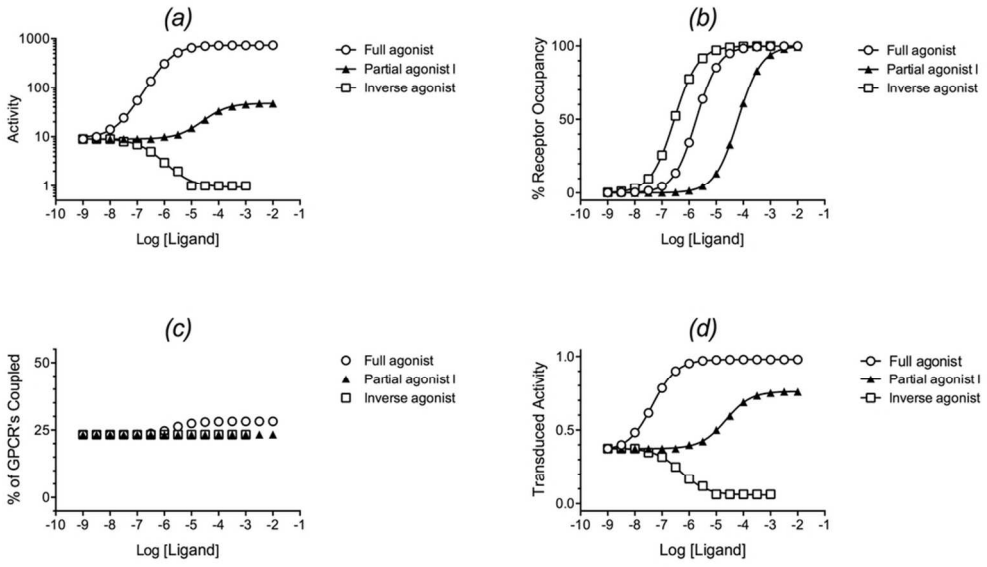

Figure 7
88x51mm (300 x 300 DPI)

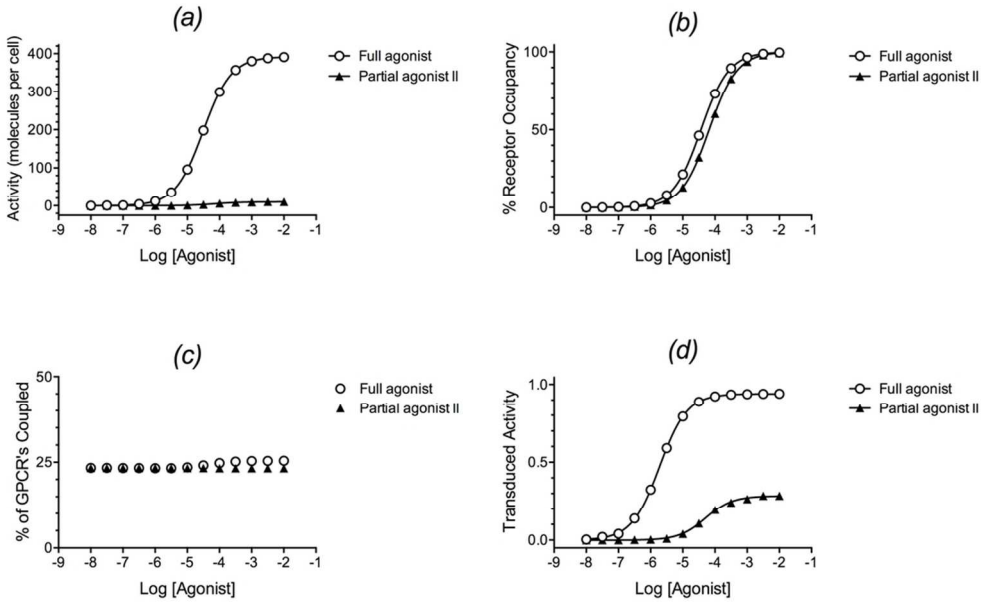

Figure 8
95x59mm (300 x 300 DPI)

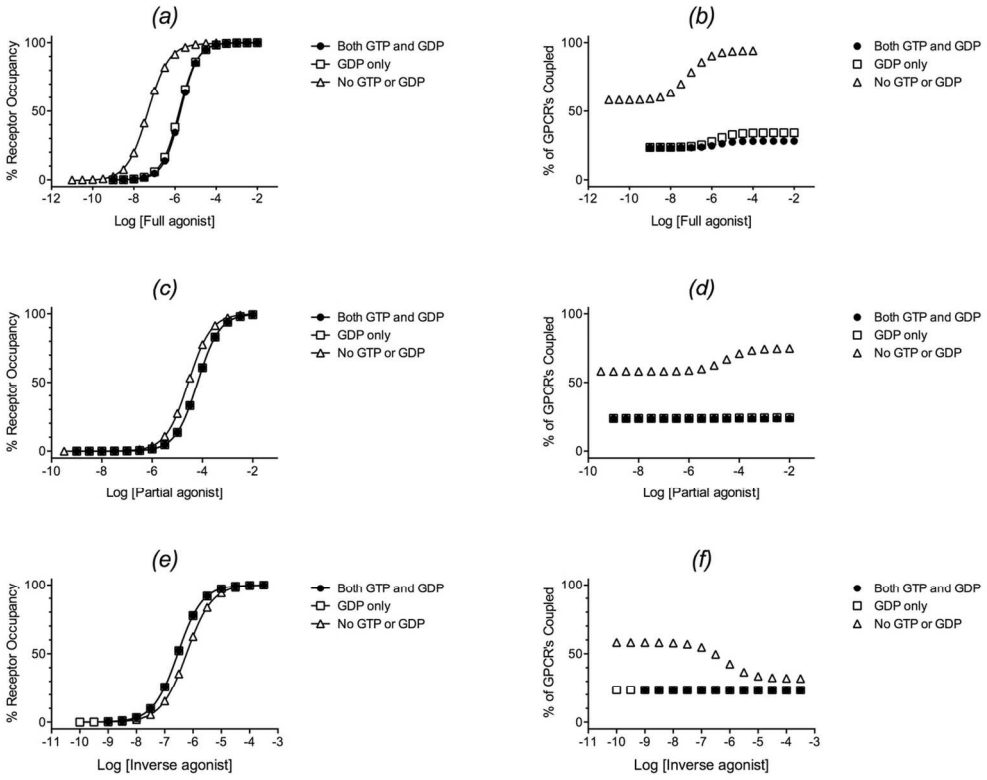

Figure 9
121x96mm (300 x 300 DPI)

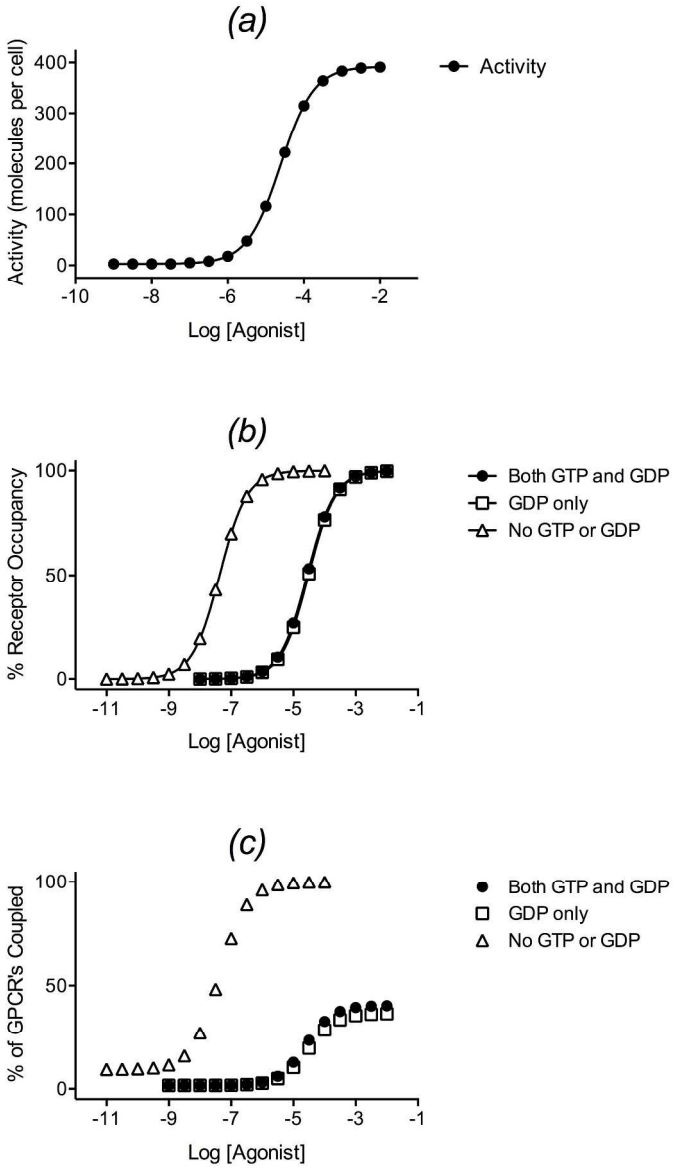

Figure 10
217x370mm (300 x 300 DPI)

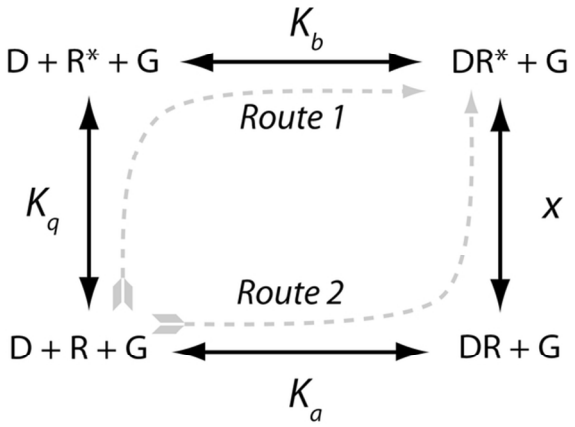

Calculations

$$K_b K_q = x K_a$$

$$x = K_b K_q / K_a$$

Figure 11
88x44mm (300 x 300 DPI)